n-body dynamics of stabilized vector solitons

Gaspar D. Montesinos
Departamento de Matemáticas, Escuela Técnica Superior de Ingenieros Industriales, Universidad de Castilla-La Mancha, 13071 Ciudad Real, Spain

María I. Rodas-Verde
Área de Óptica, Facultade de Ciencias de Ourense, Universidade de Vigo, As Lagoas s/n, Ourense, ES-32005 Spain

Víctor M. Pérez-García
Departamento de Matemáticas, Escuela Técnica Superior de Ingenieros Industriales, Universidad de Castilla-La Mancha, 13071 Ciudad Real, Spain

Humberto Michinel
Área de Óptica, Facultade de Ciencias de Ourense, Universidade de Vigo, As Lagoas s/n, Ourense, ES-32005 Spain

(Received 5 November 2004; accepted 2 June 2005; published online 21 July 2005)

In this work we study the interactions between stabilized Townes solitons. By means of effective Lagrangian methods, we have found that the interactions between these solitons are governed by central forces, in a first approximation. In our numerical simulations we describe different types of orbits, deflections, trapping, and soliton splitting. Splitting phenomena are also described by finite-dimensional reduced models. All these effects could be used for potential applications of stabilized solitons. © *2005 American Institute of Physics*. [DOI: 10.1063/1.1984807]

The cubic nonlinear Schrödinger equation (NLSE) is among the most important physical models in the field of nonlinear waves. Besides its fundamental value as a first-order nonlinear wave equation, it is an integrable model in the one-dimensional case[1] and represents many different physical systems: from laser wave packets propagating in nonlinear materials to matter waves in Bose-Einstein condensates (BEC), gravitational models for quantum mechanics, plasma physics, or wave propagation in geological systems, among others.[2–4] In this paper we consider the vector version of the NLSE and study the dynamics of some particular solutions which are stabilized by means of a periodic modulation of the nonlinearity.

I. INTRODUCTION

One of the types of NLS equations arising frequently in the applications is the two-dimensional cubic nonlinear Schrödinger equation, which is of the form

$$i\frac{\partial u}{\partial t}=\left[-\frac{1}{2}\Delta+g(t)|u|^2\right]u, \tag{1a}$$

$$u(\boldsymbol{r},0)=u_0(\boldsymbol{r})\in H^1(\mathbb{R}^2), \tag{1b}$$

where $u(\boldsymbol{r},t):\mathbb{R}^2\times\mathbb{R}^+\to\mathbb{C}$ is the complex wave amplitude, $\Delta=\partial^2/\partial x^2+\partial^2/\partial y^2$, and $g(t)$ is a real function (the nonlinear coefficient), so that if $g<0$ the nonlinearity is attractive, whereas for $g>0$ the nonlinearity is repulsive.

When g is a real constant Eq. (1a) is the cubic NLSE, which is one of the most important models of mathematical physics.

It is well known that, for $g<0$, if $N=\int_{\mathbb{R}^n}|u_0|^2$ is above a threshold value N_c, solutions of Eq. (1a) can self-focus and become singular in a finite time. This phenomenon is called *wave collapse* or *blowup of the wave amplitude*. More precisely, there is never blowup when $N<N_c$ but, for any $\epsilon>0$, there exist solutions with $N=N_c+\epsilon$ for which blowup takes place.[5,6]

Equation (1a) admits stationary solutions of the form $u(\boldsymbol{r},t)=e^{i\mu t}\Phi_\mu(\boldsymbol{r})$, where $\Phi_\mu(\boldsymbol{r})$ verifies

$$\Delta\Phi_\mu-2\mu\Phi_\mu-2g|\Phi_\mu|^2\Phi_\mu=0. \tag{2}$$

As it is precisely stated in Ref. 4, when g is negative, for each positive μ there exists only one solution of Eq. (2) which is real, positive, and radially symmetric and for which $\int|\Phi_\mu|^2d\boldsymbol{r}$ has the minimum value between all of the possible solutions of Eq. (2). Moreover, the positivity of μ ensures that this solution decays exponentially at infinity. This solution is called the *ground state* or *Townes soliton*. We will denote it as $R_\mu(r)$, which satisfies

$$\Delta R_\mu-2\mu R_\mu-2gR_\mu^3=0, \tag{3}$$

$$\lim_{r\to\infty}R_\mu(r)=0,\ R_\mu'(0)=0. \tag{4}$$

From the theory of nonlinear Schrödinger equations, it is known that the Townes soliton has exactly the critical norm for blowup N_c; therefore, it separates in some sense the region of collapsing and expanding solutions. Moreover, the Townes soliton is *unstable*, i.e., small perturbations of this solution lead to either expansion of the initial data or blowup in finite time. This instability is an essential feature of these type of equations, which has its origin in the two-

dimensional nature of the equation and makes it essentially different from its one-dimensional version, in which stable solitary-wave solutions exist, the so-called solitons.

From the physical point of view the existence of this instability implies that no localized solutions of the 2D NLSE exist. This is why there has been a great interest in the case where g is not constant but a continuous periodic function of t, which has arisen recently in different fields of applications of Eq. (1a). The intuitive idea is that (oscillating) bound states could be obtained by combining cycles of positive and negative g values so that, after an expansion and contraction regime, the solution could come back to the initial state. In this way some sort of pulsating trapped solution, i.e., a *breather*, could be obtained.

This idea was first proposed in the field of nonlinear optics.[7] In that context, a spatial modulation of the Kerr coefficient (the nonlinearity) of the optical material is used to prevent collapse so that the wave packet becomes collapsing and expanding in alternating regions and is stabilized in average.[8,9] The same idea has been used in the field of matter waves in Refs. 10 and 11. In Ref. 12 some general results are provided for generic forms of $g(t)$. Also, in Refs. 12 and 13 it has been argued that the structure which remains stabilized is a Townes soliton. The stabilization of more complex structures in the framework of Eq. (1a) constitutes an open problem, since other solutions such as those of vortex type cannot be stabilized.[8,14]

II. THE VECTOR NLS AND STABILIZED VECTOR SOLITONS

In this paper we explore the vector version of Eq. (1a), which is of the form

$$i\frac{\partial u_j}{\partial t} = -\frac{1}{2}\nabla^2 u_j + g(t)(a_{j1}|u_1|^2 + \cdots + a_{jn}|u_n|^2)u_j, \tag{5}$$

where $j=1,\ldots,n, u_j$ are the complex amplitudes $\Delta=\partial^2/\partial x^2 + \partial^2/\partial y^2, a_{jk}\in\mathbb{R}$ are the nonlinear coupling coefficients, and $g(t)$ is a periodic function accounting for the modulation of the nonlinearity.

Equation (5) is the natural extension of the Manakov system[15] to two transverse dimensions and an arbitrary number of components. In optics, for spatial solitons, t plays the role of the propagation coordinate and u_j are n mutually incoherent laser wave packets. One-dimensional Manakov-type models have been extensively studied in nonlinear optics, mainly due to the potential applications of Manakov solitons in the design of all-optical computing devices.[16] In BEC these equations (with an additional trapping term) describe the dynamics of multicomponent two-dimensional condensates, u_j being the wave functions for each of the atomic species involved.[17,18]

Some features of this model have been described in Ref. 19. In particular, it is clear that if $u_j(\mathbf{r},0)=R_\mu(\|\mathbf{r}-\mathbf{r}_j\|)$, where R_μ is a *stabilized Townes soliton* (STS), and the centers of the distributions are much more separated than the width of the Townes solitons, then we may have states with STS on each component. Because of the Galilean invariance we can also construct solutions propagating with uniform velocity along straight trajectories $\mathbf{r}_j(t)$. Again, if the trajectories are well separated it is reasonable to expect that (as it happens in the case of generic time-independent nonlinearities[20,21]) the STS will propagate without interactions. The purpose of this paper is to provide a first systematic exploration of collisions of STS. A few results were already reported in Ref. 19. One of the main contributions of that paper was to realize that, for a given set of parameters a_{jk}, it is possible to use STS to build explicit solutions of Eq. (5). These solutions are constructed by taking

$$u_j = \alpha_j R_\mu(r), \quad j=1,\ldots,n \tag{6}$$

for any set of coefficients α_j satisfying

$$a_{j1}\alpha_1^2 + \cdots + a_{jn}\alpha_n^2 = 1, \quad j=1,\ldots,n. \tag{7}$$

These solutions of Eq. (5) are called *stabilized vector solitons*(SVS) because they correspond to solutions with appreciable overlapping of the different components u_j. In Ref. 19 the stability of these structures, as well as the way they arise from collisions between stabilized solitons, was studied.

In this paper we present many more examples of collisions between STS and the associated phenomenology.

III. EFFECTIVE-PARTICLE MODEL FOR COLLISIONS OF STABILIZED TOWNES SOLITONS

A. Motivation

Before describing the direct numerical simulations of Eq. (5) in detail, and the many different phenomenologies observed, we first present an effective-particle model for collisions of STS. This model will give us a few hints on the expected dynamics of the system. The idea, as in many other problems in physics, is to assume that during the collisions stabilized solitons behave as particles in the sense that can be described qualitatively by a bell-type ansatz with a few free parameters.

This type of assumption allows us to reduce the dynamics to a finite number degrees of freedom and receives many different names depending on the field of application: method of collective coordinates, averaged Lagrangian description, time-dependent variational method, effective-particle method, etc.

In our case we take as trial Gaussian functions, which is one of the standard choices

$$u_j = A_j \exp\left[-\frac{(x-x_j)^2}{2w_{jx}^2} - \frac{(y-y_j)^2}{2w_{jy}^2} + i(v_{jx}x + v_{jy}y + \beta_{jx}x^2 + \beta_{jy}y^2)\right]. \tag{8}$$

The t-dependent parameters have the following meaning: A_j is the wave function amplitude; x_j, y_j are the coordinates of the centroid; w_{jx}, w_{jy} are the widths along the x and y axis; v_{jx}, v_{jy} the initial velocities and β_{jx}, β_{jy} are phase factors which are required to obtain reliable results.[22] Although Gaussians do not have the same asymptotic decay as STS, our choice simplifies the calculations while leading to the same qualitative relations for the parameters and, as we

will see below, the resulting equations provide an elegant and simple picture for the dynamics of the centroids of the STS.

B. Equations for the effective-particle parameters

Equation (5) can be derived by means of a variational formalism from a Lagrangian density which can be written as a sum of the Lagrangians for the linear operators plus the nonlinear interaction in the following simple form:

$$\mathcal{L} = \frac{1}{2}\sum_{j,k=1}^{n} (\mathcal{L}_j + \mathcal{L}_{jk}), \tag{9a}$$

$$\mathcal{L}_j = i(u_j \dot{u}_j^* - u_j^* \dot{u}_j) + |\nabla u_j|^2, \tag{9b}$$

$$\mathcal{L}_{jk} = g(t) a_{jk} |u_j|^2 |u_k|^2. \tag{9c}$$

The standard calculations of the method[23] consist of minimizing the trial functions from Eq. (8) over the Lagrangian density given by Eqs. (9). The final result is a set of second-order ordinary differential equations for the evolution of the effective-particle parameters. In the case of the centroids we obtain

$$\ddot{x}_j = -\sum_{k=1}^{n} \frac{\partial I_{jk}}{\partial x_j}, \tag{10a}$$

$$\ddot{y}_j = -\sum_{k=1}^{n} \frac{\partial I_{jk}}{\partial y_j}. \tag{10b}$$

With $j \neq k$ these equations are in the form of Newton's second law with I_{jk} playing the role of a potential ruling the interaction between pairs of solitons according to the expression:

$$I_{jk} = \frac{a_{jk} N_k g(t)}{\pi} \frac{e^{-[(x_k - x_j)^2]/[w_{jx}^2 + w_{kx}^2]}}{\sqrt{w_{jx}^2 + w_{kx}^2}} \frac{e^{-[(y_k - y_j)^2]/[w_{jy}^2 + w_{ky}^2]}}{\sqrt{w_{jy}^2 + w_{ky}^2}}, \tag{11}$$

$N_k = \int |u_k|^2 dx\, dy$ being the square norm of the kth wave packet. The corresponding widths along x and y are determined by the following equations:

$$\ddot{w}_{jx} = \frac{1}{w_{jx}^3} - \sum_{k=1}^{n} \frac{\partial I_{jk}}{\partial w_{jx}}, \tag{12a}$$

$$\ddot{w}_{jy} = \frac{1}{w_{jy}^3} - \sum_{k=1}^{n} \frac{\partial I_{jk}}{\partial w_{jy}}. \tag{12b}$$

Finally, some complementary relationships (first integrals of motion) for the velocities and phase coefficients are also obtained

$$v_{jx} = \dot{x}_j - 2x_j \beta_{jx}, \tag{13a}$$

$$v_{jy} = \dot{y}_j - 2y_j \beta_{jy}, \tag{13b}$$

$$\beta_{jx} = \frac{\dot{w}_{jx}}{2w_{jx}}, \tag{13c}$$

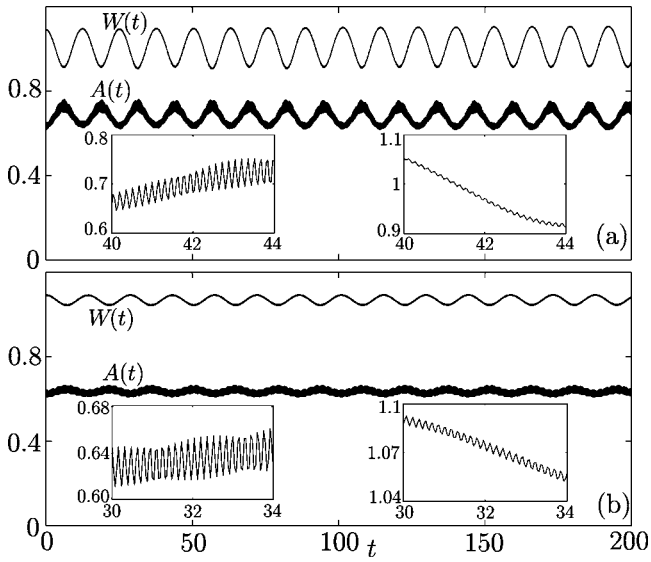

FIG. 1. Evolution of the width $W=[\int(x^2+y^2)|u|^2]^{1/2}$ and of the peak amplitude $A=\max|u|$ of the numerical solution of Eq. (5) for $n=1$ with a nonlinear coefficient (a) $g(t)=-2\pi+8\pi\cos(40t)$; (b) $g(t)=-2\pi+9.5\pi\cos(40t)$. Insets show details of the fast oscillations for the amplitude (left panel) and for the width (right panel).

$$\beta_{jy} = \frac{\dot{w}_{jy}}{2w_{jy}}. \tag{13d}$$

From Eqs. (13), it is evident that the quantities v_{jx}, v_{jy} play the role of the initial velocities of the distribution centroids.

C. Fast modulation approximation

In this paper we take the modulation $g(t)=g_0+g_1\cos\Omega t$, although the same qualitative results are obtained with other choices for g. To get STS the period of $g(t)$ must be very short[7,12,13] and the mean value $\langle g\rangle$ must satisfy the relation $\langle g\rangle < -N_c$, where N_c is the critical square norm for blowup. The oscillations of the wave packet widths, induced by $g(t)$, are very fast compared with the dynamics of the centroids ruled by the potential from Eq. (11) with an effective range of the order of the sizes of the wave packets. Therefore, as a first approximation, the evolution of x_j and y_j can be decoupled from the oscillations of ω_{jx} and ω_{jy}. With these assumptions the interaction between different wave packets will be determined by a constant nonlinearity with $g=\langle g\rangle=g_0$.

On the other hand, the parameters of the modulation can be chosen to minimize the amplitude of the wave packet oscillations.[13] An example can be seen in Fig. 1, where the results of direct numerical integrations of Eq. (5) in the one-component case $n=1$ are shown. The peak amplitude and width of the solution present a small variation when suitable parameters are taken. Thus, as a first approximation we can consider wave packets of constant circular section $w_{jx}(t)=w_{jy}(t)=w_j$. With all these considerations the potential between pairs of solitons is given by

$$I_{jk}^0 = \frac{a_{jk}N_k g_0}{\pi w^2} e^{-r_{jk}^2/w^2}, \tag{14}$$

where $w^2 = w_j^2 + w_k^2$ and r_{jk} is the distance between centroids.

Therefore, the interaction between two stabilized solitons is governed, in a first approximation, by an attractive force which only depends on the distance r_{jk} between the centroids. That is, the motion of the centroids will be similar to planetary mechanics, with a "gravitational" potential I_{jk}^0 decaying as a Gaussian instead as $1/r$. In fact, several common properties of central forces like conservation of angular momentum and the reduction of the two-body problem to a single-body motion in the center of mass frame are straightforwardly derived. Specifically, the reduced particle moves under the action of an effective potential given by

$$V = \frac{a_{jk}N_k g_0}{\pi w^2} e^{-r^2/w^2} + \frac{J^2}{2r^2} \tag{15}$$

where $g_0 < 0$ and J is the conserved angular momentum.

Using elementary techniques it is easy to obtain a necessary condition for the existence of circular orbits, namely

$$C\Delta^2 = e^{\Delta}, \tag{16}$$

where $C = 2a_{jk}N_k|g_0|/\pi J^2$ is a constant of motion and $\Delta = r^2/w^2$. If $C < e^2/4$ Eq. (16) has no solutions. If $C = e^2/4$ there is only one ($\Delta_0 = 2$), and for $C > e^2/4$ there are two solutions ($\Delta_s < \Delta_0$ and $\Delta_u > \Delta_0$). This means that, depending on the initial velocity of the wave packets v_0, two closed orbits can exit. The most internal one ($r_s < \sqrt{2}w$) is stable, whereas the external one ($r_u > \sqrt{2}w$) is unstable. If v_0 is increased up to a threshold value v_f (escape velocity) there exists only one unstable closed orbit ($r_0 = \sqrt{2}w$). Finally, if $v_0 > v_f$ closed orbits are not possible because the wave packets move too fast to be captured.

Keeping this simple picture in mind, in the next section we will perform a numerical exploration of the dynamics of stabilized solitons. Our main interest will be to check the existence of orbits and other dynamical processes.

IV. NUMERICAL SIMULATIONS OF STABILIZED SOLITON COLLISIONS

In this section we study the collisions of STS in the framework of Eq. (5). We take initial data of the form

$$u_j(\mathbf{r},0) = R_{0.5}(\|\mathbf{r} - \mathbf{r}_j\|) e^{i\mathbf{v}_j \cdot \mathbf{r}}, \tag{17}$$

and study their evolution by means of a Fourier pseudospectral scheme for the discretization of the spatial derivatives combined with a second-order split-step scheme to compute the time evolution.[13] The scheme incorporates absorbing boundary conditions to get rid of the small amounts of radiation which are generated both by the STS and the collisional processes. This type of boundary condition may be included in Eq. (5) as a complex term[13,24,25] which must be chosen to maximize the absorption of the radiation while minimizing the effect on trapped structures.

Now, we proceed to describe the different behaviors observed.

A. Fast collisions

As it was shown in Ref. 19, when "fast collisions" of STS take place the solitons emerge with only slight variations of their amplitudes and widths. For head-on collisions of two STS with initial velocities v_1 and v_2, the regime of fast collisions occurs in the range $|v_2 - v_1| > 3$ approximately.[19] These behaviors can be accounted for by the effective-particle model proposed in Sec. III. To see this, we focus on the collisions of two stabilized solitons initially placed at $\mathbf{r}_1 = (x_1, y_1)$, $\mathbf{r}_2 = (x_2, y_2)$ with initial velocities $\mathbf{v}_1 = (v_{1x}, v_{1y})$, $\mathbf{v}_2 = (v_{2x}, v_{2y})$. Following the results of Sec. III and assuming trial Gaussian functions of equal size ($w_{1x} = w_{2x} = w_x$, $w_{1y} = w_{2y} = w_y$), we obtain the equations for the effective-particle parameters

$$\ddot{x}_1 = -\frac{Ng(t)}{2\pi w_x^3 w_y} e^{-[(\ell_x^2/2w_x^2)+(\ell_y^2/2w_y^2)]} \ell_x, \tag{18a}$$

$$\ddot{x}_2 = -\ddot{x}_1, \tag{18b}$$

$$\ddot{y}_1 = -\frac{Ng(t)}{2\pi w_x w_y^3} e^{-[(\ell_x^2/2w_x^2)+(\ell_y^2/2w_y^2)]} \ell_y, \tag{18c}$$

$$\ddot{y}_2 = -\ddot{y}_1, \tag{18d}$$

$$\ddot{w}_x = \frac{1}{w_x^3} + \frac{Ng(t)}{2\pi w_x^2 w_y}\left[1 + e^{-[(\ell_x^2/2w_x^2)+(\ell_y^2/2w_y^2)]}\left(1 - \frac{\ell_x^2}{w_x^2}\right)\right], \tag{18e}$$

$$\ddot{w}_y = \frac{1}{w_y^3} + \frac{Ng(t)}{2\pi w_x w_y^2}\left[1 + e^{-[(\ell_x^2/2w_x^2)+(\ell_y^2/2w_y^2)]}\left(1 - \frac{\ell_y^2}{w_y^2}\right)\right], \tag{18f}$$

where $\ell_x = x_2 - x_1$ and $\ell_y = y_2 - y_1$. Moreover, we have the complementary relations (13) and the conservation law $N(t) = \pi|A|^2\omega_x\omega_y = \pi|A(0)|^2\omega_x(0)\omega_y(0)$. The different terms in Eqs. (18) account for the phenomenology observed in fast collisions. For example, Eqs. (18e) and (18f) contain the factors $(1 - \ell_{x,y}^2/w_{x,y}^2)$, reflecting the fact that the width evolutions depend on the separation of both solitons along the corresponding axes. One example of this kind of interaction can be seen in Fig. 2, where we plot the results of numerical simulation of Eq. (5) with $\mathbf{r}_1 = (-6, -6)$, $\mathbf{r}_2 = (6, -6)$, $\mathbf{v}_1 = (5/2^{1/2}, 5/2^{1/2})$, $\mathbf{v}_2 = (-5/2^{1/2}, 5/2^{1/2})$. Note that the time at which solitons collide is $t_c = 1.68$. In this figure we also compare the results from Eq. (5) with those obtained from Eqs. (18). We can see that, although there are quantitative differences, the effective-particle model reproduces the observed dynamics and the qualitative behavior of the system during the whole collision process.

B. Collapsing orbits

In this subsection and the following one, we have studied the evolution of two stabilized solitons which are initially placed at some points with initial velocities along the y axis, equal in absolute value but having opposite signs. If the initial velocities of the solitons are below a threshold value v_t,

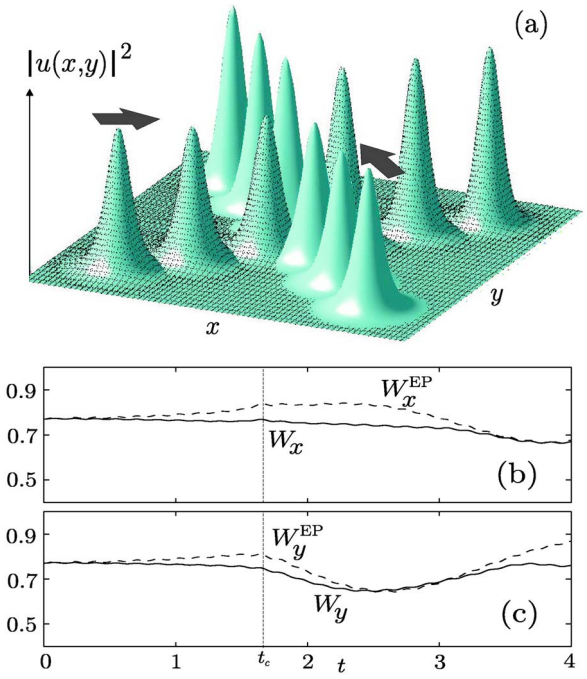

FIG. 2. (Color online). (a) Surface plots of $|u_1|^2$ and $|u_2|^2$ for times from $t=0$ to $t=3.4$ corresponding to the numerical simulation of Eq. (5) with $g(t)=-2\pi+8\pi\cos(40t)$, $\boldsymbol{r}_1=(-6,-6)$, $\boldsymbol{r}_2=(6,-6)$, $\boldsymbol{v}_1=(5/2^{1/2},5/2^{1/2})$, and $\boldsymbol{v}_2=(-5/2^{1/2},5/2^{1/2})$. (b) and (c) show the comparison of the evolution of the widths calculated numerically (solid line) and from the effective-particle model (dashed line) using Eqs. (18). The dashed vertical line indicates the time $t_c=1.68$ at which solitons collide.

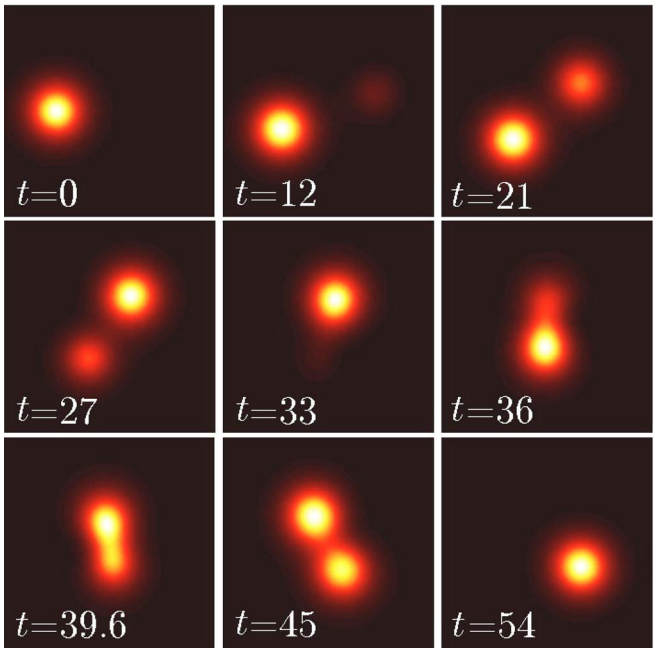

FIG. 3. (Color online). Pseudocolor plots of $|u_1|^2$ for different times corresponding to the simulation of Eq. (5) with $g(t)=-2\pi+8\pi\cos(40t)$, $\boldsymbol{r}_1=(-2,0)$, and $v_{1y}=-0.06$. During the evolution the solution is moving in a counterclockwise direction.

the mutual attraction dominates during the evolution and the solitons move inward on a spiraling orbit. For the case $\boldsymbol{r}_1=(-2,0)$ and $\boldsymbol{r}_2=(2,0)$ we have calculated numerically this threshold velocity and found it to be $v_t=0.079$. An example of this kind of orbit can be seen in Fig. 3 and Fig. 4, where we plot the evolution of $|u_1|^2$ and $|u_2|^2$ for different times when the input velocities are $v_{1y}=-0.06$ and $v_{2y}=0.06$. We have found that the interaction between solitons provokes a splitting of the wave packets as those described in Ref. 19: each soliton splits into two parts so that two stabilized vector solitons are generated. The fraction of one individual soliton distributed in the two parts is changing continuously due to the mutual interaction between the two wave packets. It is important to understand that each vector soliton is formed by one part of one soliton and another part of the other soliton; these two parts overlapped during evolution. The distance between the centroids of the two vector solitons decreases monotonically until they join at the origin at $t=35$, approximately. Then, they repel and the process starts again. Notice that the evolution of both components u_1 and u_2 is symmetrical with respect to the axis perpendicular to the line joining the two components. It is remarkable that the solitons are continuously readjusting their form in such a way that a delicate balance of both components is satisfied in order to avoid the collapse (as those reported in Ref. 26 for a different model) or the spreading of these structures.

The effective-particle method cannot take into account the readjustment phenomenon between stabilized solitons observed in Fig. 3 and Fig. 4. Therefore, this simplified description is not valid anymore and can be used only as a first approximation to the problem. A more sophisticated model will be presented in Sec. V.

C. Expanding orbits

For initial velocities larger than the critical value v_t, it is possible to overcome the collapsing character of the orbit

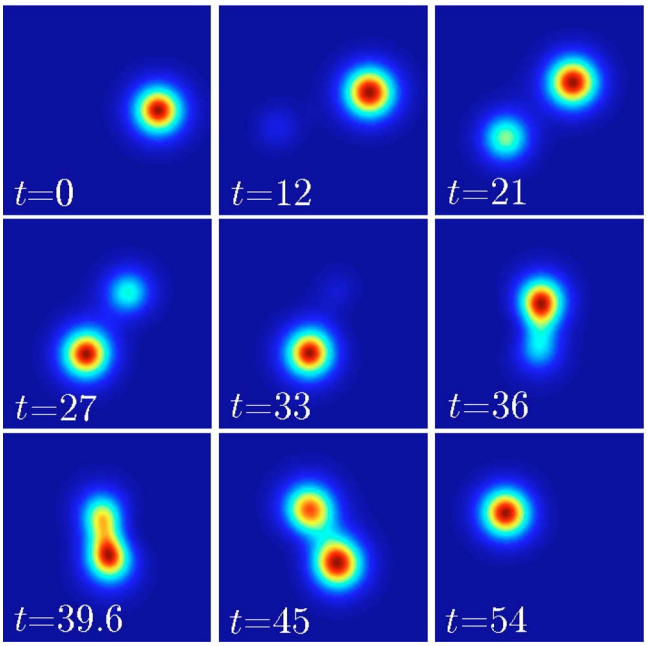

FIG. 4. (Color online). Same as Fig. 4 for the evolution of component u_2 with $\boldsymbol{r}_2=(2,0)$ and $v_{2y}=0.06$. As in Fig. 3, the solution is moving in a counterclockwise direction.

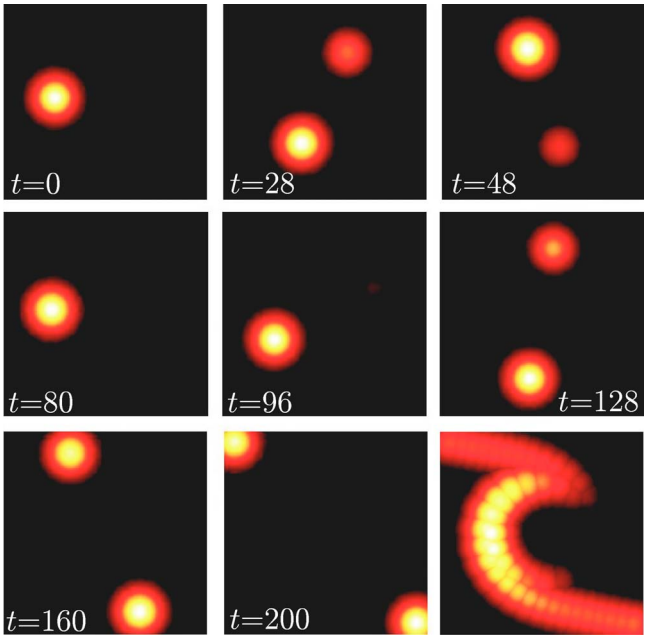

FIG. 5. (Color online). Pseudocolor plots of $|u_1|^2$ for different times corresponding to the evolution of component u_1 from simulation of Eqs. (5) with $g(t)=-2\pi+8\pi\cos(40t)$, $\boldsymbol{r}_1=(-2,0)$, and $v_{1y}=-0.08$. The last picture corresponds to the superposition of several snapshots from $t=0$ to $t=200$. Again, the solution is moving in a counterclockwise direction.

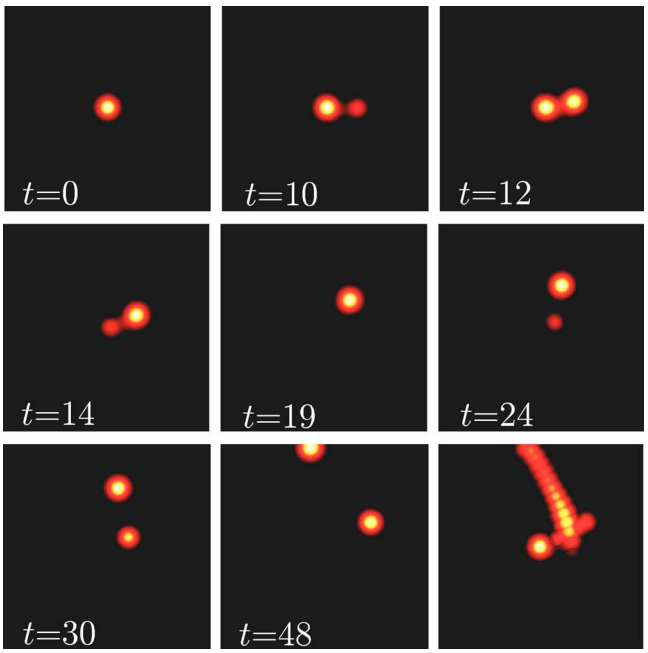

FIG. 7. (Color online). Pseudocolor plots of $|u_1|^2$ for different times corresponding to the evolution of component u_1 from simulation of Eq. (5) with $g(t)=-2\pi+8\pi\cos(40t)$, $\boldsymbol{r}_1=(0,0)$, and $\boldsymbol{v}_1=0$. The last pseudocolor plot corresponds to the superposition of several snapshots from $t=0$ to $t=50$. It is also shown as a surface plot in the bottom-right picture.

and the stabilized solitons follow outward trajectories. In Fig. 5 and Fig. 6 we show the results obtained for two stabilized solitons initially placed at $\boldsymbol{r}_1=(-2,0)$ and $\boldsymbol{r}_2=(2,0)$ with input velocities $v_{1y}=-0.08$ and $v_{2y}=0.08$ along the y axis.

Again, we observe the formation of SVS. Since what is plotted is the amplitude of only one component ($|u_1|^2$ or $|u_2|^2$), the existence of two main spots in many subplots of Fig. 5 and Fig. 6 show, once more, that the interaction between stabilized solitons not only affects their trajectories, but also induces a readjustment of the individual distributions and the dynamical formation of SVS. We will try to describe this phenomenon in the next section.

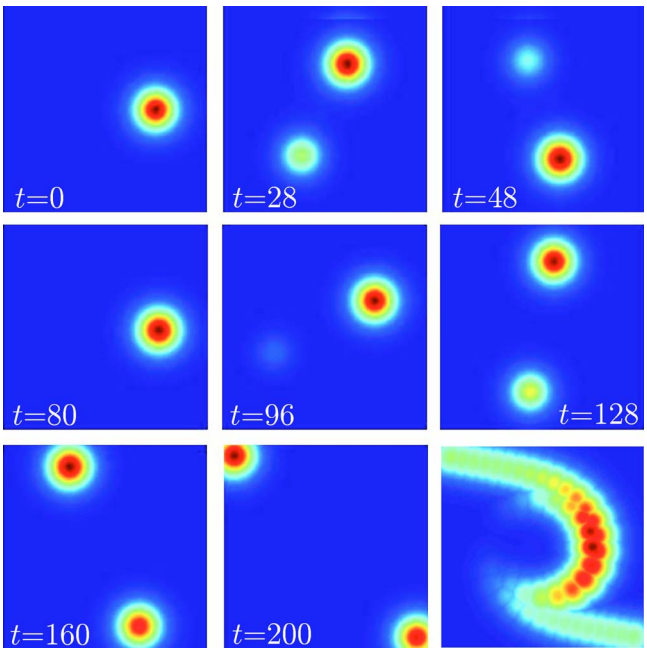

FIG. 6. (Color online). Same as Fig. 5 for the evolution of component u_2 with $\boldsymbol{r}_2=(2,0)$ and $v_{2y}=0.08$.

D. Wave packet splitting with deflection

In this section we consider another interesting case: one stabilized soliton initially at rest and another one approaching it. The situation is shown in Fig. 7 and Fig. 8, where we plot, respectively, the evolution of u_1 and u_2. The first wave packet starts at $\boldsymbol{r}_1=(0,0)$ with zero initial velocity and the second one is initially placed at $\boldsymbol{r}_2=(3,-3)$ with initial velocity $v_{2y}=0.3$ along the y axis. It can be appreciated how the interaction leads to the formation of SVS by means of the same splitting mechanism observed in previous figures. Pictures show that both wave packets split simultaneously and part of u_1 is dragged by one half of u_2 forming a vector soliton. The remaining vector soliton is deflected.

E. Three interacting solitons

We have also studied the three-body problem, which corresponds to three solitons in the corners of an equilateral triangle of side d. Therefore, by taking the origin of coordinates in the barycenter the solitons are placed at $\boldsymbol{r}_1=(0,d/\sqrt{3})$, $\boldsymbol{r}_2=(-d/2,-d/2\sqrt{3})$, $\boldsymbol{r}_3=(d/2,-d/2\sqrt{3})$. The initial velocities are $v_{1x}=-v\sin(\pi/2)$, $v_{1y}=0$, $v_{2x}=-v\sin(\pi/2+2\pi/3)$, $v_{2y}=v\cos(\pi/2+2\pi/3)$, $v_{3x}=-v\sin(\pi/2+4\pi/3)$, and $v_{3y}=v\cos(\pi/2+4\pi/3)$ being v the input velocity. The numerical results for $d=4$ and $v=0.12$ are shown in Fig. 9, where we see the evolution of one of the wave packets. The

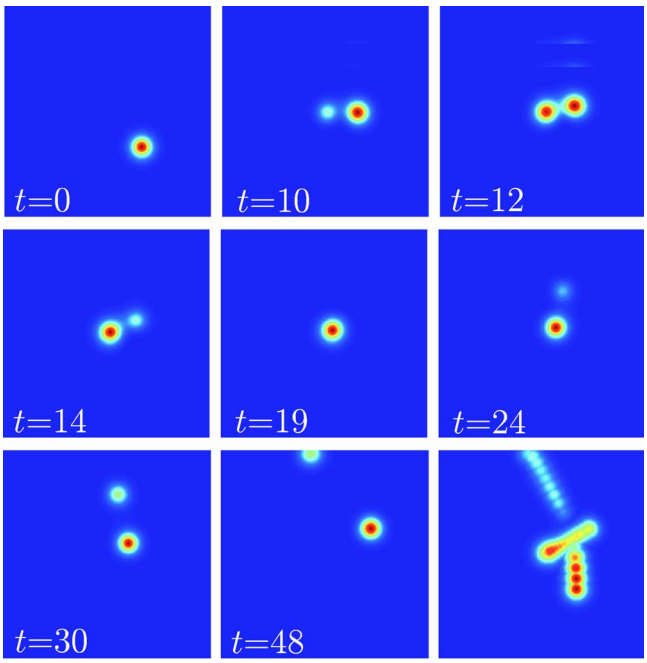

FIG. 8. (Color online). Same as Fig. 7 for the evolution of component u_2 with $\boldsymbol{r}_2=(3,-3)$ and $v_{2y}=0.3$.

initial velocities are such that the attraction between solitons is not enough to keep them bounded and the wave packets move outward. As in the previous cases the distributions split during evolution, the initial distributions readjust due to the interaction with the other two components, and three two-part vector solitons are generated.

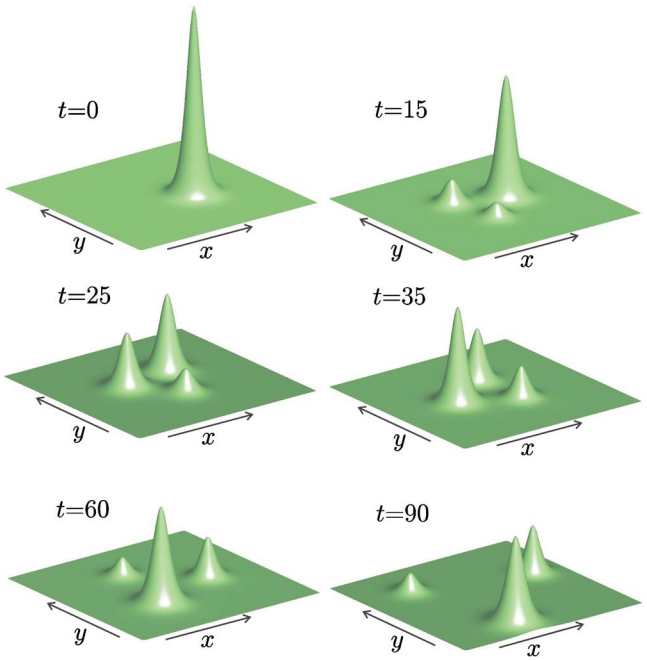

FIG. 9. (Color online). Surface plots of $|u_3|^2$ for different times corresponding to the evolution of component u_3 from simulation of Eq. (5) with $\boldsymbol{r}_1=(0,d/\sqrt{3})$, $\boldsymbol{r}_2=(-d/2,-d/2\sqrt{3})$, $\boldsymbol{r}_3=(d/2,-d/2\sqrt{3})$ and initial velocities $v_{1x}=-v\sin(\pi/2)$, $v_{1y}=0$, $v_{2x}=-v\sin(\pi/2+2\pi/3)$, $v_{2y}=v\cos(\pi/2+2\pi/3)$, $v_{3x}=-v\sin(\pi/2+4\pi/3)$, $v_{3y}=v\cos(\pi/2+4\pi/3)$ $d=4$, being $v=0.12$, and $g(t)=-2\pi+8\pi\cos(40t)$.

V. THEORETICAL ANALYSIS OF THE WAVE PACKET SPLITTING

A. Motivation and Ansatz

From the previous section it is clear that the effective-particle model used in Sec. III cannot explain the wave packet splitting observed in most of our numerical simulations. Therefore, in this section we develop another approach to capture the main characteristics of such splitting. We will use again an effective Lagrangian technique, but now we consider a two-mode model described by the following Ansätze:

$$u_1 = A_{11}\exp\left[-\frac{(x-\ell)^2}{2w_{1x}^2}-\frac{y^2}{2w_{1y}^2}\right] + A_{12}\exp\left[-\frac{(x+\ell)^2}{2\tilde{w}_{1x}^2}-\frac{y^2}{2\tilde{w}_{1y}^2}\right], \tag{19a}$$

$$u_2 = A_{21}\exp\left[-\frac{(x-\ell)^2}{2w_{2x}^2}-\frac{y^2}{2w_{2y}^2}\right] + A_{22}\exp\left[-\frac{(x+\ell)^2}{2\tilde{w}_{2x}^2}-\frac{y^2}{2\tilde{w}_{2y}^2}\right], \tag{19b}$$

where the t-dependent parameters $A_{ij}, i,j=1,2$ are complex quantities including the wave amplitude and a phase which can give rise to a phase difference between components. This choice now allows readjustment of mass between two parts related to each component of the vector system, i.e., u_1 is now composed of two parts which can be used to emulate the splitting mechanism and the formation of SVS.

However, the full analysis of Eqs. (19) by effective Lagrangian methods is cumbersome; to achieve some results we will make several simplifications which can be justified by the observation of the simulations. In the first place, when the initial stabilized solitons u_1 and u_2 are equal, the splitting mechanism is a symmetric process, meaning that the growth rate of one part of u_1 is the same as that of the growth rate of the corresponding part of u_2. Therefore, we can consider $A_{11}=A_{22}=\alpha$, $A_{12}=A_{21}=\beta$, $w_{1x}=\tilde{w}_{2x}$, $w_{1y}=\tilde{w}_{2y}$, $\tilde{w}_{1x}=w_{2x}$, $\tilde{w}_{1y}=w_{2y}$. Second, we will assume that the sizes of every part are very similar and remain close to their mean values except for the fast oscillations. So, we consider that $w_{1x}=w_{2x}=\tilde{w}_{1x}=\tilde{w}_{2x}=w_x$ and $w_{1y}=w_{2y}=\tilde{w}_{1y}=\tilde{w}_{2y}=w_y$, w_x, w_y being constants.

Finally, to get some insight into the problem we consider the case where the distance between centroids 2ℓ is approximately constant, which can happen for instance during a fast switching process. Thus, the only free parameters are α and β.

B. Model equations

The Lagrangian $L=\int\mathcal{L}dx\,dy$ obtained from the density Lagrangian $\mathcal{L}$ given by Eqs. (9) when the Ansätze are as in Eqs. (19) is

$$L = \pi w_x w_y \Bigg\{ i(\alpha\dot{\alpha}^* - \alpha^*\dot{\alpha} + \beta\dot{\beta}^* - \beta^*\dot{\beta}) + i(\alpha\dot{\beta}^* - \alpha^*\dot{\beta} + \beta\dot{\alpha}^* - \beta^*\dot{\alpha})e^{-l^2/w_x^2} + (|\alpha|^2 + |\beta|^2)\left(\frac{1}{2w_x^2} + \frac{1}{2w_y^2}\right) + (\alpha\beta^* + \beta\alpha^*)\left(\frac{w_x^2 - 2l^2}{2w_x^4} + \frac{1}{2w_y^2}\right)e^{-l^2/w_x^2} + \frac{g(t)}{2}\{(|\alpha|^4 + |\beta|^4)[1 + e^{-2l^2/w_x^2}] + [6|\alpha|^2|\beta|^2 + 2(\alpha^2(\beta^*)^2 + (\alpha^*)^2\beta^2)]e^{-2l^2/w_x^2} + 2|\alpha|^2|\beta|^2 + 4(|\alpha|^2 + |\beta|^2)(\alpha\beta^* + \alpha^*\beta)e^{-3l^2/2w_x^2}\}\Bigg\}, \tag{20}$$

where we have taken $a_{11}=a_{12}=a_{21}=a_{22}=1$.

The standard calculations[23] yield to a system of ordinary differential equations for α and β

$$\begin{pmatrix} 1 & e^{-\ell^2/w_x^2} \\ e^{-\ell^2/w_x^2} & 1 \end{pmatrix}\begin{pmatrix} \dot{\alpha} \\ \dot{\beta} \end{pmatrix} = -\frac{i}{2}\begin{pmatrix} \Lambda_1 & \Lambda_2 \\ \Lambda_2 & \Lambda_1 \end{pmatrix}\begin{pmatrix} \alpha \\ \beta \end{pmatrix}, \tag{21}$$

where

$$\Lambda_1(t) = \frac{1}{2w_x^2} + \frac{1}{2w_y^2} + g(t)\left[\frac{2N(t)}{\pi w_x w_y}e^{-\ell^2/2w_x^2} + (|\alpha|^2 + |\beta|^2) \times (1 + e^{-2\ell^2/w_x^2} - 2e^{-\ell^2/2w_x^2})\right], \tag{22a}$$

$$\Lambda_2(t) = \left\{\frac{w_x^2 - 2\ell^2}{2w_x^4} + \frac{1}{2w_y^2} + g(t)\left[\frac{2N(t)}{\pi w_x w_y} + (|\alpha|^2 + |\beta|^2) \times (2e^{-\ell^2/2w_x^2} - 2)\right]\right\}e^{-\ell^2/w_x^2}, \tag{22b}$$

and the function $N(t)$ is the square norm of the Ansätze

$$N(t) = \|u_i\|_2^2 = \pi w_x w_y[|\alpha|^2 + |\beta|^2 + (\alpha\beta^* + \alpha^*\beta)e^{-\ell^2/w_x^2}].$$

System (21) can be written as

$$\begin{pmatrix} \dot{\alpha} \\ \dot{\beta} \end{pmatrix} = i\begin{pmatrix} \nu_1 & \nu_2 \\ \nu_2 & \nu_1 \end{pmatrix}\begin{pmatrix} \alpha \\ \beta \end{pmatrix}, \tag{23}$$

where

$$\nu_1(t) = \frac{\Lambda_2(t)e^{-\ell^2/w_x^2} - \Lambda_1(t)}{2(1 - e^{-2\ell^2/w_x^2})}, \tag{24a}$$

$$\nu_2(t) = \frac{\Lambda_1(t)e^{-\ell^2/w_x^2} - \Lambda_2(t)}{2(1 - e^{-2\ell^2/w_x^2})}. \tag{24b}$$

Using system (23) and its complex conjugate, and taking into account that $\nu_1, \nu_2 \in \mathbb{R}$, can be immediately proved that

$$\frac{d}{dt}(|\alpha|^2 + |\beta|^2) = 0, \tag{25a}$$

$$\frac{d}{dt}(\alpha\beta^* + \alpha^*\beta) = 0, \tag{25b}$$

and therefore three invariants exist

$$|\alpha|^2 + |\beta|^2 = q_0, \tag{26a}$$

$$\alpha\beta^* + \alpha^*\beta = q_1, \tag{26b}$$

$$N(t) = N_0, \tag{26c}$$

q_1, q_2, N_0 being constants.

System (23) can be solved numerically to find the evolution of the amplitudes α and β. Nevertheless, we can solve it analytically by considering that ν_1 and ν_2 are constants, since the only dependence on t is given by the nonlinear coefficient $g(t)$ and, as we discussed in Sec. III C, the dynamics is determined by an averaged nonlinearity $g=g_0$. By writing $\alpha=\alpha_R+i\alpha_I$, $\beta=\beta_R+i\beta_I$ with α_R, α_I, β_R, $\beta_I \in \mathbb{R}$, the solutions of system (23) are obtained by using basic techniques from the theory of ordinary differential equations. The result is

$$\begin{pmatrix} \alpha_R \\ \beta_R \\ \alpha_I \\ \beta_I \end{pmatrix} = \frac{1}{2}M\begin{pmatrix} \sin(\nu_1 - \nu_2)t \\ \cos(\nu_1 - \nu_2)t \\ \sin(\nu_1 + \nu_2)t \\ \cos(\nu_1 + \nu_2)t \end{pmatrix}, \tag{27}$$

where

$$M = \begin{pmatrix} -M_1 & M_2 & -M_3 & M_4 \\ M_1 & -M_2 & -M_3 & M_4 \\ M_2 & M_1 & M_4 & M_3 \\ -M_2 & -M_1 & M_4 & M_3 \end{pmatrix}, \tag{28}$$

and

$$M_1 = \alpha_I(0) - \beta_I(0), \tag{29a}$$

$$M_2 = \alpha_R(0) - \beta_R(0), \tag{29b}$$

$$M_3 = \alpha_I(0) + \beta_I(0), \tag{29c}$$

$$M_4 = \alpha_R(0) + \beta_R(0), \tag{29d}$$

$\alpha_R(0)$, $\alpha_I(0)$, $\beta_R(0)$, $\beta_I(0)$ being the initial conditions.

C. Validation

Taking as initial conditions $\alpha_R(0)=\alpha_0$, $\alpha_I(0)=\beta_R(0)=\beta_I(0)=0$ from Eq. (27), we obtain

$$\alpha_R = \alpha_0 \cos\nu_1 t \cos\nu_2 t, \tag{30a}$$

$$\beta_R = -\alpha_0 \sin\nu_1 t \sin\nu_2 t, \tag{30b}$$

$$\alpha_I = \alpha_0 \sin\nu_1 t \cos\nu_2 t, \tag{30c}$$

$$\beta_I = \alpha_0 \cos\nu_1 t \sin\nu_2 t, \tag{30d}$$

and the amplitude evolutions are straightforwardly derived

$$|\alpha| = \alpha_0|\cos\nu_2 t|, \tag{31a}$$

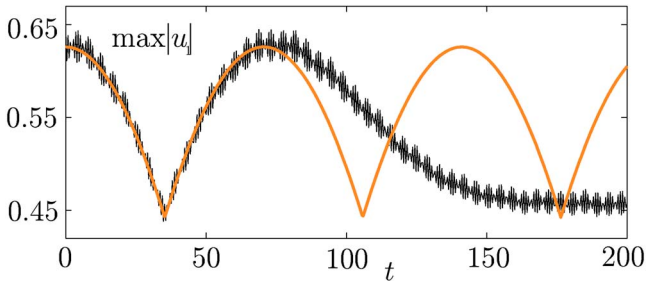

FIG. 10. Comparison of the evolution of the peak amplitude of the wave packet u_1 corresponding to the simulation of Fig. 5 and Fig. 6, obtained by direct numerical simulation of Eq. (5) with the periodic oscillations from Eqs. (31) predicted by the wave packet splitting model.

$$|\beta| = \alpha_0 |\sin \nu_2 t|. \tag{31b}$$

Equations (31) mean that the splitting mechanism is oscillatory and periodic, as can be seen in Figs. 3–8. In Fig. 10 we compare the evolution of the peak amplitude of the wave packet u_1 corresponding to the simulation of Fig. 5 and Fig. 6 (for which $\ell=2$), obtained by direct numerical simulation of Eq. (5) with Eqs. (31). The value of ν_2 is calculated according to Eq. (24b) with a slight correction in the value of ℓ, which is taken as $\ell=1.88$. This correction is due to the fact that numerical simulations of Fig. 5 and Fig. 6 are made with Townes solitons intial data, whereas the analysis of the wave packet splitting is made under the assumption of Gaussian initial data. Therefore, since Townes solitons decay at infinity as $\exp(-r)$ and Gaussians do at $\exp(-r^2)$, for a fixed separation 2ℓ, the overlapping between Townes solitons is greater than between Gaussians. For these reasons, to compare both situations it is necessary to take a smaller value of ℓ in the case of Gaussian data. We see that there is a very good agreement between both curves up to around $t=70$. After that, numerical simulations show that solitons repel each other and the theoretical analysis is not valid anymore, because we supposed constant separation between solitons. Therefore, we can conclude that our two-mode model is valid to predict the readjustment of mass between the wave packets provided that the distance between parts remains nearly constant. As in the one-dimensional case, the final repulsion of the wave packets can be explained by taking into account that the relative phases between coherent solitons tend to separate them.[27] In this case, the solution of Eq. (30) gives a phase difference which takes the values $\pm\pi/2$.

Finally, we must notice that the formation of vector solitons is the dominant tendency of the system in the slow collision regime. Therefore, the effective-particle model must be combined with the analysis of the partial splitting in order to get a more accurate picture of the dynamics. In fact, this kind of soliton exhibits a teleportation behavior as they suddenly vanish to appear in another place. This effect is very fast and can have potential applications in optical information processing.

VI. CONCLUSIONS

In this paper, we have presented a detailed study of interactions between wave packets which are stabilized against collapse by means of a modulation of the nonlinear term, i.e., stabilized solitons.

We have studied their dynamics by direct numerical simulations of the model equations. In this study, we have found that the system presents collapsing and expanding orbits depending on the initial configuration as well as other phenomena as deflection of one wave packet due to the attraction and split in several parts in the corresponding n-body interactions.

We have also developed a theoretical explanation of the wave packet splitting based on effective Lagrangian methods, and corroborated that effective-particle models allow one to obtain conclusions for this system only in very limited situations. It is important to point out that some approximate general methods have been developed in previous works (see Refs. 28 and 29) to find an effective potential of interaction between far separated solitons both in scalar and vector systems when the nonlinear coefficient is constant. In our case, however, the fact that the nonlinear coefficient is a function of time and that the solitons are interacting leading to the formation of complex structures makes a similar approach not valid for our work.

ACKNOWLEDGMENTS

G. D. M. and V. M. P-G. are partially supported by Ministerio de Educación y Ciencia under Grant BFM2003-02832 and Consejería de Educación y Ciencia of the Junta de Comunidades de Castilla-La Mancha under Grant PAC-02-002. G. D. M. acknowledges support from Grant AP2001-0535 from MECD.

[1] V. E. Zakharov and A. B. Shabat, "Exact theory of two-dimensional self-focusing and one-dimensional self-modulation of waves in nonlinear media," Sov. Phys. JETP **34**, 62 (1972).
[2] N. N. Akhmediev and A. Ankiewicz, *Solitons: Nonlinear Pulses and Wavepackets* (Chapman and Hall, London, 1997).
[3] *Nonlinear Klein-Gordon and Schrödinger Systems: Theory and Applications*, edited by L. Vázquez, L. Streit, and V. M. Pérez-García (World Scientific, Singapore, 1996).
[4] C. Sulem and P. Sulem, *The Nonlinear Schrödinger Equation: Self-focusing and Wave Collapse* (Springer, Berlin, 2000).
[5] G. Fibich and G. Papanicolaou, "Self-focusing in the perturbed and unperturbed nonlinear Schrödinger equation in critical dimension," SIAM J. Appl. Math. **60**, 183 (1999).
[6] M. I. Weinstein, "Nonlinear Scrödinger equations and sharp interpolation estimates," Commun. Math. Phys. **87**, 567 (1983).
[7] L. Berge, V. K. Mezentsev, J. J. Rasmussen, P. L. Christiansen, and Y. B. Gaididei, "Self-guiding light in layered nonlinear media," Opt. Lett. **25**, 1037 (2000).
[8] I. Towers and B. A. Malomed, "Stable (2+1)-dimensional solitons in a layered medium with sign-alternating Kerr nonlinearity," J. Opt. Soc. Am. B **19**, 537 (2002).
[9] A. Kaplan, B. V. Gisin, and B. A. Malomed, "Stable propagation and all-optical switching in planar waveguide-antiwaveguide periodic structures," J. Opt. Soc. Am. B **19**, 522 (2002).
[10] H. Saito and M. Ueda, "Dynamically stabilized bright solitons in a two-dimensional Bose-Einstein condensate," Phys. Rev. Lett. **90**, 040403 (2003).
[11] F. Abdullaev, J. G. Caputo, R. A. Kraenkel, and B. A. Malomed, "Controlling collapse in Bose-Einstein condensates by temporal modulation of the scattering length," Phys. Rev. A **67**, 013605 (2003).
[12] G. D. Montesinos, V. M. Pérez-García, and P. Torres, "Stabilization of solitons of the multidimensional nonlinear Schrödinger equation: Matter-wave breathers," Physica D **191**, 193210 (2004).
[13] G. D. Montesinos and V. M. Pérez-García, e-print arxiv.org/nlin.PS/0312020, Math. Comput. Simulat. (to be published).

[14]G. D. Montesinos, V. M. Pérez-García, H. Michinel, and J. R. Salgueiro, "Stabilized vortices in layered Kerr media," Phys. Rev. E **71**, 036624 (2005).
[15]S. V. Manakov, "On the theory of two-dimensional stationary self-focusing of electromagnetic waves," Sov. Phys. JETP **38**, 248 (1974).
[16]T. Kanna and M. Lakshmanan, "Exact soliton solutions of coupled nonlinear Schrodinger equations: Shape-changing collisions, logic gates, and partially coherent solitons," Phys. Rev. E **67**, 046617 (2003).
[17]D. S. Hall, M. R. Matthews, J. R. Ensher, C. E. Wieman, and E. A. Cornell, "Dynamics of component separation in a binary mixture of Bose-Einstein condensates," Phys. Rev. Lett. **81**, 1539 (1998).
[18]B. D. Esry and C. H. Greene, "Bose-Einstein condensates—Superfluids mixing it up," Nature (London) **392**, 434 (1998).
[19]G. D. Montesinos, V. M. Pérez-García, and H. Michinel, "Stabilized two-dimensional vector solitons," Phys. Rev. Lett. **92**, 133901 (2004).
[20]I. Rodnianski, W. Schlag, and A. Soffer, e-print arxiv.org/math.AP/0309114.
[21]G. Perelman,"Asymptotic stability of multi-soliton solutions for nonlinear Schrödinger equations," Commun. Partial Differ. Equ. **29** (7–8), A051 (2004).
[22]V. M. Pérez-García, "Self-similar solutions and collective coordinate methods for nonlinear Schrodinger equations," Physica D **191**, 211 (2004).
[23]For a review, see B. A. Malomed, Prog. Opt. **43**, 69 (2002).
[24]P. Tran, "Solving the time-dependent Schrodinger equation: Suppression of reflection from the grid boundary with a filtered split-operator approach," Phys. Rev. E **58**, 8049 (1998).
[25]T. Fevens and H. Jiang, "Absorbing boundary conditions for the Schrödinger equation," SIAM J. Comput. **21**, 255 (1999).
[26]B. B. Baizakov, B. A. Malomed, and M. Salerno, "Multidimensional solitons in a low-dimensional periodic potential," Phys. Rev. A **70**, 053613 (2004).
[27]Yu. S. Kivshar and G. P. Agrawal, *Optical Solitons: From Fibers to Photonics Crystals* (Academic Press, San Diego, 2003).
[28]B. A. Malomed, "Potential of interaction between two- and three-dimensional solitons," Phys. Rev. A **58**, 7928 (1998).
[29]A. Maimistov, B. Malomed, and A. Desyatnikov, "A potential of incoherent attraction between multidimensional solitons," Phys. Lett. A **254**, 179 (1999).